Available online at www.sciencedirect.com
ScienceDirect
Ceramics International 35 (2009) 1121–1128
CERAMICS INTERNATIONAL
www.elsevier.com/locate/ceramint

Effect of different nucleation catalysts on the crystallization of Li_2O–ZnO–MgO–Al_2O_3–SiO_2 glasses

Omar A. Al-Harbi

Natural Resource and Environment Research Institute, King Abdulaziz City for Science and Technology, P.O. Box 6086, Riyadh 11442 Saudi Arabia

Received 8 June 2007; received in revised form 5 April 2008; accepted 13 May 2008
Available online 19 July 2008

Abstract

Based on local raw materials, a range of LiZnMg aluminosilicate glasses were prepared to investigate the influence of TiO_2, Cr_2O_3, and ZrO_2 on the crystallization behaviour and thermal expansion characteristics. Differential thermal analysis showed that the crystallization propensity increases in the order $TiO_2 > Cr_2O_3 > ZrO_2$. Virgilite, β-spodumene ss, gahnite, enstatite and cristobalite were formed in the prepared glass-ceramics. The microstructure of glass-ceramic samples showed growths of rounded and subrounded grains in the base sample, whereas, somewhat rod-like and accumulated growths appeared in samples containing ZrO_2. However, a rather homogeneous texture of accumulated growths was developed in glass-ceramics containing TiO_2 and Cr_2O_3. The coefficient of thermal expansion of parent glasses was sensitive to the type of nucleating agent added ($Cr_2O_3 > TiO_2 > ZrO_2$) varying from 24.8×10^{-7} to 65.1×10^{-7} °C^{-1} being almost unchanged with the heat-treatment. The microhardness values of glass-ceramic samples were in the 763–779 kg/mm^2 range.

Keywords: D. Glass-ceramic; D. Silicate; C. Thermal expansion; Spinels; Microstructure

1. Introduction

Glass-ceramic properties depend on microstructure and composition of phases developed during the manufacturing process. The ability to control these two parameters depends on the original composition as well as the heat-treatment regime. Properties such as the coefficient of thermal expansion depend on the nature and volume of the developed phases in addition to the heat-treatment history [1].

Glass-ceramics based on Li_2O–Al_2O_3–SiO_2 (LAS) glass may form different important phases that have commercial purposes, and have therefore been the subject of many previous studies. Crystalline phases within $LiAlSi_xO_{2x-2}$ formulae can be prepared from lithium aluminosilicate glasses. Some cations, for example Mg and Zn, can substitute Li, leading to changes in the crystalline phase formulae [2,3]. In the solid solution state, crystalline phases such as β-eucryptite and β-spodumene are developed in glass-ceramic materials; however, intermediate phases may also develop [4].

In commercial LAS glass-ceramics, ZnO has been used to lower the melting point [4]. Within the crystallization of spodumene–willemite–diopside system, the TiO_2 and ZrO_2 nucleating agents influence the type, the proportions of crystalline phases, the transformation temperature and the texture of resultant glass-ceramic [5]. Crystallization of spodumene–willemite glasses formed β-eucryptite, β-spodumene and willemite and the increase of Zn leads to increase of the grain sizes and thermal expansion coefficients [6]. In presence TiO_2, a phase separation has been observed prior to nucleation and in presence ZnO or MgO allow the formation of the particularly stable of spinel titanates [7]. However, improvement in glass-ceramic took place through the nucleation and crystallization of many glass systems based on lithium aluminum silicate composition [8,9]. Recently bulk crystalline glass-ceramics was obtained from CaLi aluminosilicate glass, since both parent and Cr_2O_3-containing glasses showed enhanced crystallization of β-eucryptite and wollastonite, whereas anorthite formation was catalysed in TiO_2-containing glasses, in addition to the latter phases mentioned [10].

Zinc aluminate ($ZnAl_2O_4$) is a mineral gahnite and is a member of the spinel family. It can be used as a second phase in glaze layers of white ceramic tiles to improve wear resistance

E-mail address: oalharbi@kacst.edu.sa.

0272-8842/$34.00
doi:10.1016/j.ceramint.2008.05.008

and mechanical properties, and to preserve whiteness [11]. Zinc aluminate can also be used as a catalyst support, since it has a high thermal stability, low acidity and a hydrophobic behaviour.

The influence of TiO_2, Cr_2O_3, and ZrO_2 on the crystallization of the parent glass was investigated, as well as physical properties such as the thermal expansion coefficient and microhardness.

2. Experimental procedure

The nominal composition of the glass used in this study based on 50 mol.% Li-disilicate ($Li_2Si_2O_5$) and 50 mol.% ZnO-containing cordierite $MgZnAl_4Si_5O_{18}$. The starting materials for glass batches were local Saudi clay, magnesite, and white silica sand (Table 1). The chemical analysis of the represented raw materials has been carried out using induced coupled (ICP-MS-model ELAN 9000 PerkinElmer) at ALS Chemex Lab, Canada. Commercial Li_2CO_3 and ZnO were also added to the glass batch composition (Table 2). A range of nucleation catalysts, for example TiO_2 (3 g: GT1, 6 g: GT2), Cr_2O_3 (0.5 g: GC1, 1 g: GC2) and ZrO_2 (3 g: GZ) were added to the 100 g of glass batch oxide (Table 3).

Well-mixed powders, of either the parent glass or the nucleat-containing glass, were melted in an alumina crucible for 2 h in the 1400–1500 °C temperature range. The glass melt was quenched into a steel mould and annealed at 450 °C. The samples were subjected to varying crystallization heat-treatments, ranging from 800 to 1100 °C, at intervals 100 °C with a heating rate of 10 °C min^{-1}.

The thermal behaviour was detected, for the glass powder $<0.5 > 0.25$ mm, using a computerized differential thermal analysis (DTA, Model DTG-60H, Shimadzu, Japan) with a heating rate of 10 °C min^{-1}, under a dynamic N_2 gas flow and an alumina standard. Identification of crystalline phases in glass-ceramic samples was performed using an X-ray powder diffractometer (MiniFlex; Rigaku, Japan) using Ni-filtered and Cu Kα radiation. The obtained X-ray diffraction patterns were recorded in the 2θ range 4–70°. A step-scanning mode was employed with a step size of 0.02° and a constant time per step of 1 s. The automated data acquisition system allowed peak positioning with good accuracy, 0.02° with a maximum peak tip width of 0.087°.

Scanning electron microscope (SEM) observations (JSM-5800, Japan) were made on fresh-fractured glass-ceramic samples that had been etched with 1% HNO_3 + 1%HF acid for 30 s and coated with a thin gold film.

Table 2
Parent batch composition

Composition in wt%	
SiO_2	63.22
Al_2O_3	14.61
Fe_2O_3	3.29
MgO	5.80
ZnO	5.73
CaO	1.20
Li_2O	4.32
K_2O	0.26
Na_2O	0.92
TiO_2	0.74

Table 3
Nucleating agents

Glass no.	Nucleating agent		
	TiO_2[a]	Cr_2O_3[a]	ZrO_2[a]
G0	–	–	–
GT1	3	–	–
GT2	6	–	–
GC1	–	0.5	–
GC2	–	1.0	–
GZ	–	–	3

[a] Grams over 100 g glass oxide.

The coefficients of thermal expansion (CTE) were determined for the glass and glass-ceramic samples (dimension 0.5 cm × 0.5 cm × 2.0 cm) using a NETZSCH dilatometer (DIL 402PC, Germany) with a heating rate of 5 °C min^{-1}. Static hardness was measured using a microhardness tester (Digital Microhardness, MHV2000) with a 100 g load and 15 s dwell time. An average of five indentations was calculated for each sample.

3. Results and discussion

3.1. DTA analysis

DTA thermograms of the glass samples show that the incorporation of a nucleation catalyst considerably changes both the endothermic and exothermic peak temperatures. However, the endothermic and exothermic effects were located in the 648–730 °C and 700–980 °C temperature ranges, respectively (Fig. 1). Adding TiO_2 to the parent glass, i.e. GT1 and GT2 did not change the endothermic peak greatly; however, it decreased the main exothermic peak temperature

Table 1
Chemical analysis of the starting raw materials

Raw material	Oxides (%)								
	SiO_2	Al_2O_3	Fe_2O_3	MgO	K_2O	Na_2O	CaO	TiO_2	LOI
White silica sand	97.35	0.67	0.35	–	–	0.67	0.44	–	0.52
Clay	57.65	24.25	5.36	0.21	0.43	1.20	0.48	1.24	9.00
Magnesite	04.25	00.25	0.09	41.83	0.06	0.11	5.76	<0.05	47.7

LOI, loss on ignition.

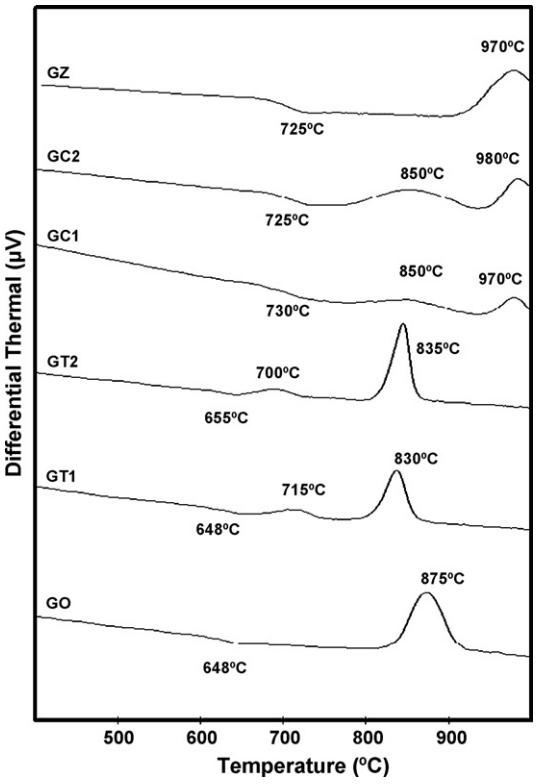

Fig. 1. DTA thermograms of the present glasses.

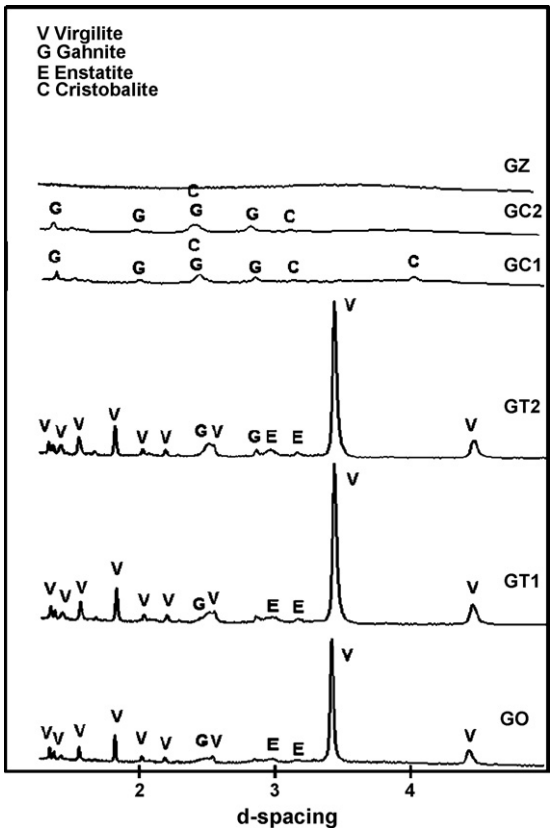

Fig. 2. X-ray diffraction patterns of the present glasses heat-treated at 800 °C/3 h.

from 875 to 830 and 835 °C, respectively (Fig. 1). Weak exothermic peaks were also detected at 715 °C (GT1) and 700 °C (GT2).

Adding Cr_2O_3 to the base glass, i.e. GC1 and GC2, increased the endothermic temperature to 730 °C and the main exothermic peaks to 980 °C. However, secondary weak exotherms were developed at 850 °C for both GC1 and GC2 samples (Fig. 1). On the other hand, GZ parent glasses containing ZrO_2 have the same thermal behaviour of GC1 but with an intense exothermic peak and an absence of any secondary peak (Fig. 1).

It must be mentioned that the DTA curves show that the parent glass doped with either Cr_2O_3 or ZrO_2 have a higher crystallization temperature than the glass doped with TiO_2. From the exothermic peaks and the X-ray analysis (below), the order of crystallization was $TiO_2 > Cr_2O_3 > ZrO_2$. This may reflect the influence of these nucleation catalysts on this parent glass system.

3.2. X-ray analysis

The X-ray diffraction patterns of the crystallized glasses are shown in Figs. 2–5 and in Table 4.

Crystalline phases developed in these glasses were virgilite (β-quartz ss, $Li_xAl_xSi_{3-x}O_6$), gahnite ($ZnAl_2O_4$), Li–aluminium silicate (β-spodumene, $LiAlSi_2O_6$), enstatite ($Fe_{.093}Mg_{.907}Fe_{.405}Mg_{.595}Si_2O_6$) and cristobalite. The added nucleation catalysts played an important role in the phase change as well as the developed textures.

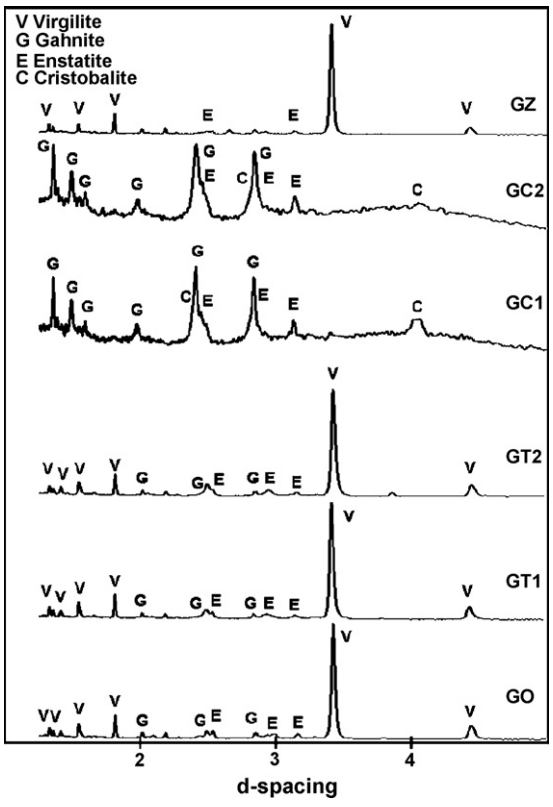

Fig. 3. X-ray diffraction patterns of the present glasses heat-treated at 900 °C/3 h.

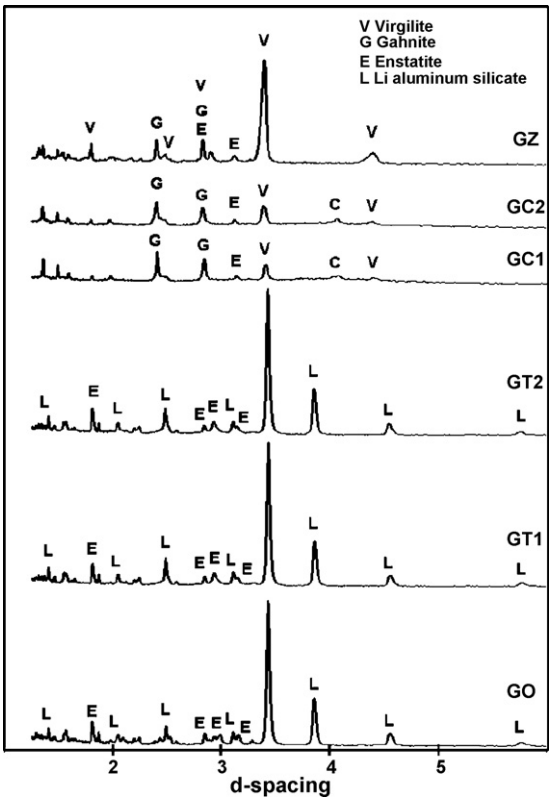

Fig. 4. X-ray diffraction patterns of the present glasses heat-treated at 1000 °C/3 h.

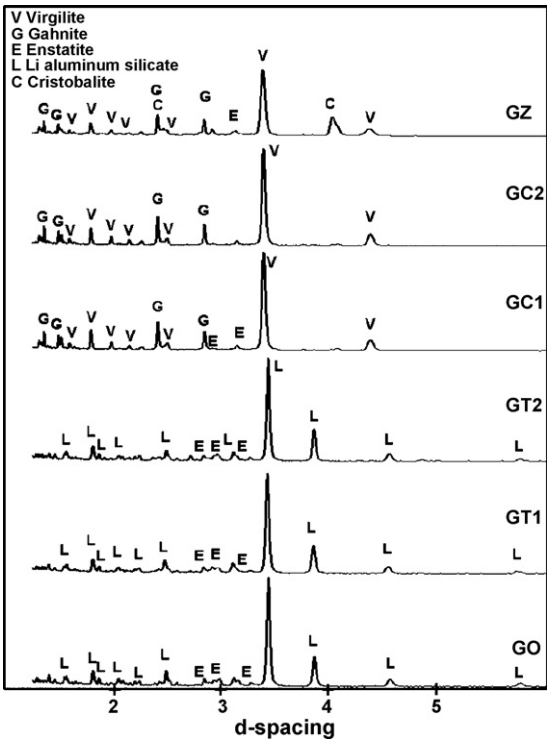

Fig. 5. X-ray diffraction patterns of the present glasses heat-treated at 1100 °C/3 h.

Following a heat-treatment at 900 °C for 3 h, virgilite with traces of enstatite were developed in the parent G0 glass or the TiO_2-containing GT1 and GT2 samples, however, traces of gahnite were also detected (Fig. 3). Increasing the heat-treatment temperature to over 900 °C promoted the development of β-spodumene ss in preference to virgilite, whilst enstatite continued to develop and gahnite disappeared (compare Figs. 4 and 5). This means that, at higher temperatures, the possible substitution of Mg and Zn for Li alters virgilite $Li_xAl_xSi_{3-x}O_6$ into MgZn-containing Li–aluminium silicate or β-spodumene ss. The absence of gahnite at higher temperature may support such substitution. Also at higher temperatures, an increase of enstatite content took place (Figs. 4 and 5).

On the other hand, incorporation of Cr_2O_3 in the parent glass slightly enhanced gahnite and cristobalite at 800 °C in the form of traces (Fig. 2). However, gahnite becomes the main phase with enstatite and cristobalite at 900 °C. Increasing the temperature to 1000 °C showed the appearance of virgilite with traces of cristobalite in addition to the later phases, i.e. Zn-spinel gahnite and enstatite (Fig. 4). At 1100 °C, gahnite disappeared and virgilite became the main phase along with enstatite with traces of cristobalite (Fig. 5).

Incorporation of ZrO_2 in the GZ glass delayed crystallization, which began at 900 °C with formation of virgilite, with traces of enstatite. At higher temperatures (1000 °C or 1100 °C) virgilite still the major phase and appearance of gahnite, enstatite and cristobalite took place (Figs. 4 and 5).

The results described here demonstrate the control of nucleation catalysts on phase formation and transformation. Although the Li–aluminosilicate phases were enhanced at temperatures up to 900 °C by addition of both TiO_2 and ZrO_2 as nucleation catalysts, gahnite was the main phase with a Cr_2O_3 catalyst. Virgilite is the major phase at high temperatures (1100 °C) with Cr_2O_3 and ZrO_2 catalysts, but it is converted into aluminosilicate or β-spodumene in the parent and TiO_2-catalysed glasses. Gahnite may have become the main phase in the 900–1000 °C range in the Cr_2O_3-containing samples.

The previous glass-ceramic work based on ZnO–Li_2O–Al_2O_3–SiO_2 system cleared that in case of ZnO 2–5 wt%, formation of gahnite was secondary and the β-quartz ss was the main phase [12]. Other similar work with high ZnO percent (16–40 wt%), the authors mentioned that, presence of ZrO_2 lead to the primary phase separation of ZrO_2 followed by formation β-quartz ss and gahnite formed at high temperature. However, with addition of TiO_2 a nanosized gahnite was the primary crystal phase and transparent glass-ceramic was obtained [13]. Gahnite ($ZnAl_2O_4$) or spinel ($MgAl_2O_4$) glass-ceramic was also developed, using $ZrO_2$and/or TiO_2, within SiO_2–Al_2O_3–ZnO–MgO glass [14].

The composition of naturally occurring virgilite is very similar to that of β-spodumene. Substitution of Mg^{2+} and Zn^{2+} for Li^+ may cause relatively rapid transformation of virgilite to β-spodumene, therefore significant amounts of Mg^{2+} and Zn^{2+} are possible in virgilite. During prolonged heating, Zn–gahnite was precipitated [15]. Beall and Duke [16] refer to this crystalline phase as β-quartz solid solution since it is isostructural with β-quartz. Petzoldt and Pannhorst [17]

Table 4
The developed crystalline phases at different temperatures

Sample no.	Heat-treatment parameter (°C/h)	Developed phases	Sample morphology
G0	–	A	Transparent dark brown glass
	800/3	V–E(t)	Translucent gray smooth surface with grayish core
	900/3	V–E–G(t)	Light green opaque, surface with grayish core
	1000/3	L–E(t)	Light brown opaque with grayish core
	1100/3	L–E (t)	Light brown opaque with grayish core
GT1	–	A	Transparent dark brown glass
	800/3	V–E(t)	Translucent gray smooth surface with grayish core
	900/3	V–E–G(t)	Opaque Gray surface with grayish core
	1000/3	L–E(t)	Dark brown opaque with grayish core
	1100/3	L–E (t)	Dark brown opaque with grayish core
GT2	–	A	Transparent dark brown glass
	800/3	V–E(t)	Translucent gray smooth surface with grayish core
	900/3	V–G(t)	Gray surface opaque with grayish core
	1000/3	L–E(t)	Light creamy surface opaque with grayish core
	1100/3	L–E (t)	Light creamy surface opaque with grayish core
GC1	–	A	Transparent dark green glass
	800/3	G(t)–C(t)	Translucent light brown chocolate
	900/3 1000/3	G–E–C	Opaque, light brown chocolate
	1100/3	V–G–E–C(t)	Opaque, light brown chocolate
		V–E–C(t)	Opaque, light brown chocolate
GC2	–	A	Transparent dark green glass
	800/3	G(t)–C(t)	Light brown, bulk translucent chocolate
	900/3	G–E–C	Opaque, light brown chocolate
	1000/3	V–G–E(t)–C(t)	Opaque, light brown chocolate
	1100/3	V–E–C(t)	Opaque, light brown chocolate
GZ	–	A	Transparent black glass
	800/3	A	Dark brown, bulk translucent with light brown core
	900/3	V–E(t)	Opaque, light brown chocolate
	1000/3	V–G–E–C	Opaque, light brown chocolate
	1100/3	V–G–E	Opaque, light brown chocolate

A, amorphous; V, virgilite (JCPDS card 31–707); L, Li–aluminum silicate; β-spodumene (35–794), G, gahnite (JCPDS card 5–669); E, enstatite ferroan (JCPDS card 83–666); C, cristobalite (JCPDS card 39–1425); t, trace.

suggested the following formula for this β-quartz solid solution, with a possible incorporation of the $AlPO_4$ structural unit:

$$Li_{2-2(v-w)}Mg_vZn_wO\,Al_2O_3\,xAlPO_4\,(y-2x)SiO_2$$

In the parent and TiO_2-containing glasses, virgilite transformed into β-spodumene ss with increasing enstatite content at high temperatures (>900 °C). Therefore, Zn-containing β-spodumene ss became the dominant phase. In glass-containing Cr_2O_3, virgilite appeared at higher temperatures (>900 °C) and did not transform into β-spodumene. However, Cr_2O_3 enhanced production of ZnO-gahnite, which was the dominant phase at low temperatures. As with the Cr_2O_3 catalyst, glass-containing ZrO_2 did not transform virgilite into β-spodumene.

3.3. Microstructure

The microstructure of the glass-ceramics prepared after heat-treatment at 900 °C, mainly comprised crystals of virgilite or gahnite in a cryptocrystalline groundmass (Fig. 6). The G0 parent glass-ceramic shown in Fig. 6 the growth of rounded to subrounded crystals (∼1–5 μm). Finer grains (<1–2.5 μm) appeared in the sample-containing TiO_2, whereas distinct rod-like and rounded crystals were found in the sample-containing ZrO_2. Somewhat homogeneous textures of accumulated granular growths (<1–2.5 μm) were developed in crystallized samples containing Cr_2O_3.

Generally, the TiO_2 and Cr_2O_3 nucleating agents showed the most effective production of nearly homogeneous glass-ceramic. This may be due to glass-in-glass phase separation promoted by the presence of dopant nuclei upon which the dominant phase can grow [18]. This dominant phase consisted of virgilite (β-quartz ss) and gahnite samples containing TiO_2 and Cr_2O_3. Formation of spinel or gahnite acts as a nucleant in glass-containing Cr_2O_3, especially, when Cr^{3+} enters the spinel structure [19], this lead to the development of almost homogeneous microstructures.

3.4. CTE and V′H measurements

The CTE values of the present glass-ceramics were between 24.91 and 65.66 × 10^{-7} °C^{-1} at 25–520 °C temperature range (Table 5 and Fig. 7). The value of CTE is very sensitive to the type and contents of added nucleant, however, the Cr_2O_3-

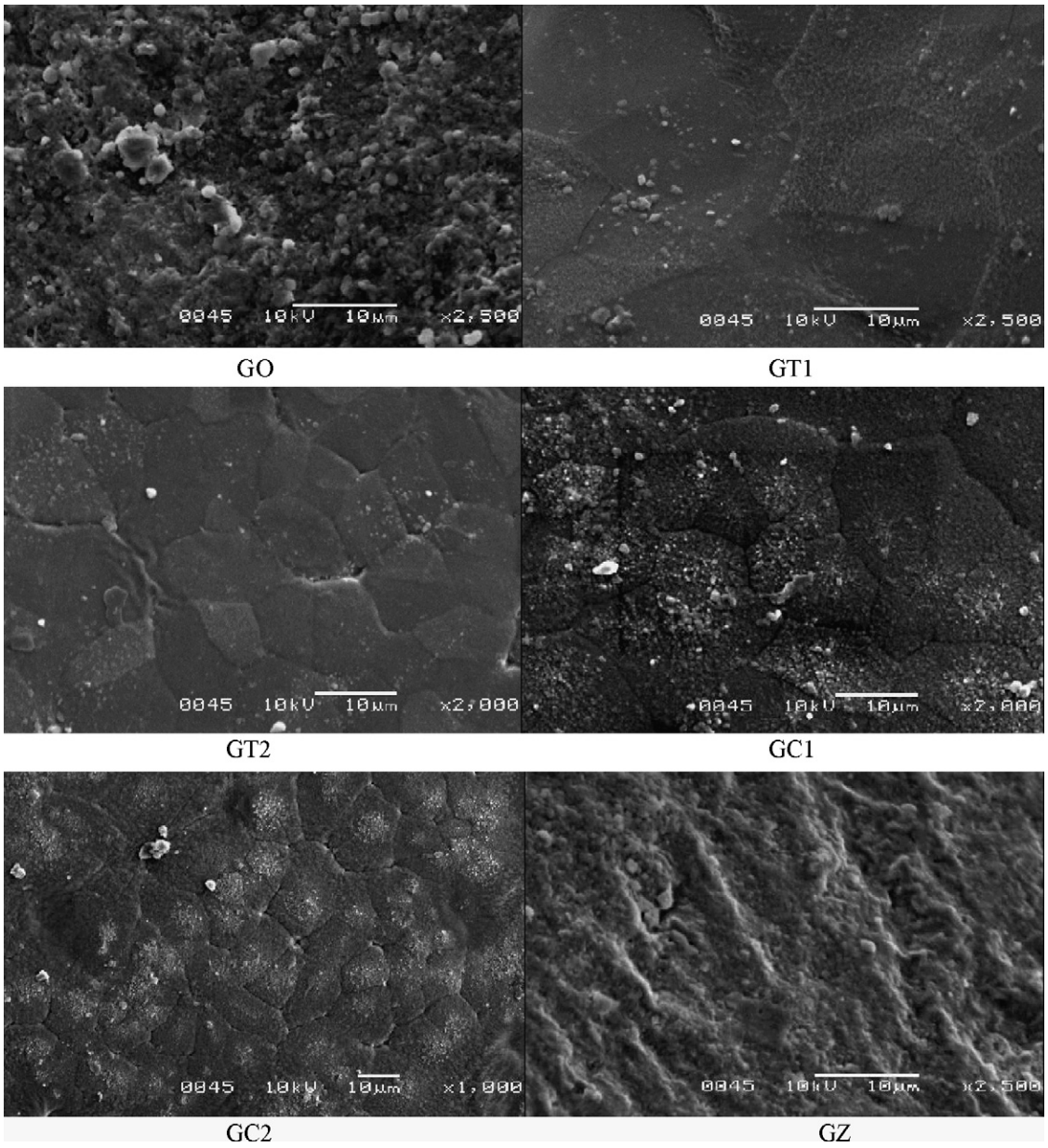

Fig. 6. SE micrographs of the present glasses heat-treated at 900 °C/3 h.

Table 5
CTE and V′H values of the present samples

Glass no.	CTEα × 10^{-7} °C^{-1} (25–520 °C)		Microhardness V′H value kg/mm^2	Developed phases
	α-Value	Heat-treatment (°C/h)		
G0	24.81	–	–	A
	25.61	900/3	738	V–E(t)–G(t)
GT1	27.44	–	–	A
	24.91	900/3	765	V–E(t)–G(t)
GT2	27.44	–	–	A
	27.93	900/3	763	V–E(t)–G(t)
GC1	59.99	–	–	A
	60.71	900/3	790	G–E–C
GC2	65.06	–	–	A
	65.66	900/3	787	G–E–C
GZ	34.89	–	–	A
	35.65	900/3	779	V–E(t)

A, amorphous; V, virgilite; G, gahnite; E, enstatite ferron; C, cristobalite; t, trace.

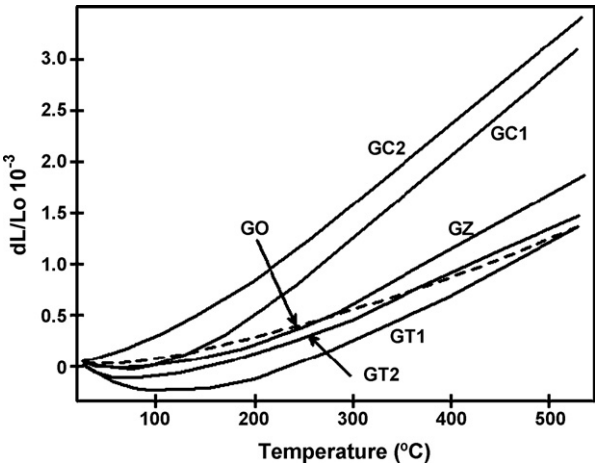

Fig. 7. CTE of the present glasses.

containing samples have the highest value, whereas, base- and TiO_2-containing glasses have the lowest value. The CTE curves of the corresponding glass-ceramic samples are shown in Fig. 8 and Table 5. The CTE values depend mainly on the formed phases as well as the residual glass.

Table 5 reveals that dominance of virgilite in the G0, GT1, GT2 and GZ samples lead to low CTE values (24.91–35.65 × 10^{-7} °C^{-1} in the 25–520 °C range). If Zn–gahnite dominates with enstatite and cristobalite, the CTE was high (60.71–65.66 × 10^{-7} °C^{-1} in the 25–520 °C range) in both GC1 and GC2 samples.

In the pseudoquaternary SiO_2–$LiAlO_2$–$MgAl_2O_4$–$ZnAl_2O_4$-system, previous studies have shown that the CTE decreases with increasing Li_2O and ZnO and increases with increasing Mg [13]. In the present study, the CTE value increased to 65.66 × 10^{7} °C^{-1} in the 25–520 °C range in glass-ceramics containing Cr_2O_3 when either crystallization of spinel occurred (i.e. Zn–gahnite was the main phase) or enstatite was present with cristobalite. However, dominance of virgilite in ZrO_2-containing glass-ceramics decreased the CTE to 35.65 × 10^{-7} °C^{-1} in the 25–520 °C range.

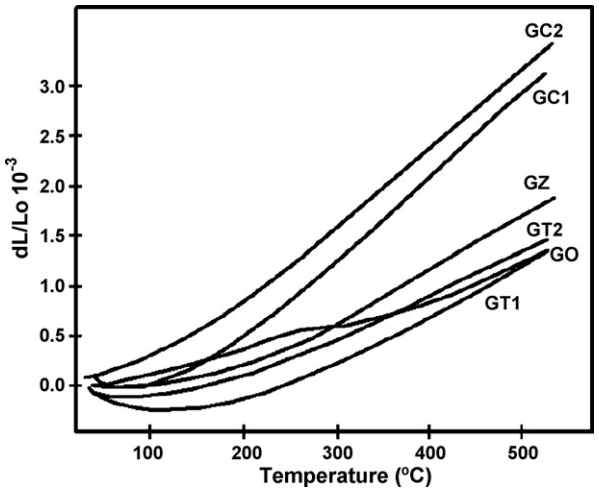

Fig. 8. CTE of the present glasses heat-treated at 900 °C/3 h.

The microhardness values of glass-ceramic samples were in the 763–779 kg/mm^2 range but were higher in the sample-containing gahnite, enstatite, and cristobalite (Table 5).

4. Conclusion

In this study, transparent glasses were obtained in the Li_2O–ZnO–MgO–Al_2O_3–SiO_2 system, using TiO_2, Cr_2O_3 and ZrO_2 as nucleation catalysts. For these three catalysts, early crystallization occurred in the order $TiO_2 > Cr_2O_3 > ZrO_2$. Virgilite (or β-quartz ss), β-spodumene ss, gahnite, enstatite and cristobalite were developed by varying the heat-treatment. Rounded and subrounded grains developed in the base sample, whilst rod-like and rounded accumulated growths appeared in samples containing ZrO_2. A reasonably homogeneous texture comprising rounded and subrounded grains developed in the samples containing TiO_2 and Cr_2O_3. The Coefficient of thermal expansion of parent glasses was sensitive to the type of nucleating agent added ($Cr_2O_3 > TiO_2 > ZrO_2$) varying from 24.8 × 10^{-7} to 65.1 × 10^{-7} °C^{-1} being almost unchanged with the heat-treatment. Crystallization of virgilite, with traces of enstatite, gave a low CTE value (24.91–27.93 × 10^{-7} °C^{-1}) in parent or TiO_2-containing samples, whilst crystallization of a very low ratio of enstatite in sample-containing ZrO_2 leads to an intermediate CTE value (35.65 × 10^{-7} °C^{-1}). In samples containing Cr_2O_3, the absence of virgilite, and dominance of Zn–gahnite with enstatite and cristobalite resulted in a relatively high CTE value (60.71–65.66 × 10^{-7} °C^{-1}). The microhardness values of glass-ceramic samples were in the 763–779 kg/mm^2 range but were higher in the sample-containing gahnite, enstatite, and cristobalite.

Acknowledgments

The author gratefully acknowledges the support of the king Abdulaziz City for Science and Technology (KACST) for funding the research project BM-24-01 entitled ‘‘Investigation and development of local raw materials for production of glass and glass-ceramics’’ on which the paper is based. I thank to the project’s consultant Dr. Esmat Hamzawy (National Research Center-Egypt) for his valuable comments and ideas that helped to improve the paper. Also thanks to Dr. M.M. Khan for helping in field and lab work.

References

[1] W. Höland, G. Beall, Glass-Ceramic Technology, The American Ceramic Society, Westerville, OH, USA, 2002, 43081.
[2] W. Pannhorst, Overview, in: H. Bach (Ed.), Low Thermal Expansion Glass Ceramics, Springer-Verlag, Berlin, 1995, pp. 1–12.
[3] J. Petzoldt, Metastabile mischkristalle mit quatzstructur im oxide system Li_2O–MgO–ZnO–Al_2O_3–SiO_2, Glastechn. Ber. 40 (1967) 385–396.
[4] M. Guedes, A.C. Ferro, J.M.F. Ferreira, Nucleation and crystal growth in commercial LAS compositions, J Eur. Ceram. Soc. 21 (2001) 1187–1194.
[5] A.W.A. El-Shennawi, A.A. Omar, A.M. Morsi, The role of titania and titania mixtures in the nucleation and crystallization of spodumene–willemite–diopside glasses, Thermochim. Acta 58 (1982) 125–153.

[6] Hua.F A.M., M. Lia, D.L. Mao Dali a, K.M. Liang, Crystallization and properties of a spodumene–willemite glass ceramic, Thermochim. Acta 437 (2005) 110–113.
[7] L. Barbieri, A. Bonamartini Corradi, C. Leonelli, C. Silgardi, T. Manfredini, G.C. Pellacani, Effect of TiO_2 on the properties of complex aluminosilicate glasses and glass-ceramics, Mater. Res. Bull. 32 (6) (1997) 637–648.
[8] A.W.A. El-Shennawi, E.M.A. Hamzawy, G. Khater, A.A. Omar, Crystallization of some aluminosilicate glasses, Ceram. Int. 27 (2001) 725–730.
[9] C. Kangguo, Carbon effect on crystallization kinetics of Li_2O–Al_2O_3–SiO_2 glasses, J. Non-Cryst. Solid 238 (1998) 152–157.
[10] O.A. Al-Harbi, Influence of TiO_2 and Cr_2O_3 on the crystallinity and properties of CaLi aluminosilicate glass, Adv. Appl. Ceram. 106 (5) (2007) 235–240.
[11] A. Escardino, S.J. LAmoro, A. Gozalbo, M.J. Orts, A. Moreno, Gahnite: devitrification in ceramic frits—mechanism and kinetics, J. Am. Ceram. Soc. 83 (2000) 2938–2944.
[12] G.H. Beall, L.R. Pinckney, Variable translucent glass-ceramic article and method for making (1992), Eur. Pat. No. EP 0 536 478 02.07.92.
[13] Z. Strnad, Glass-ceramic Materials, Glass Science and Technology, 8, Elsevier, 1986.
[14] G.H. Beall, L.R. Pinckney, Nanophase glass-ceramics, J Am. Ceram. Soc. 82 (1999) 5–16.
[15] D.U. Tulyaganov, S. Agathopoulos, H.R. Fernandes, J.M.F. Ferreira, Synthesis of lithium aluminosilicate glass and glass-ceramics from spodumene material, Ceram. Int. 30 (2004) 1023–1030.
[16] G.H. Beall, D.A. Duke, Transparent glass-ceramics, J. Mater. Sci. 4 (1969) 340–352.
[17] J. Petzoldt, W. Pannhorst, Chemistry and structure of materials for high precision optical applications, J. Non-Cryst. Solids 129 (1991) 191–198.
[18] G.H. Beall, in: I. Birkby (Ed.), Ceramic Technology International, Sterling Publication Ltd., London, England, 1992, pp. 89–93.
[19] V. Poncon, V. Kalisky, G. Boulon, R. ReisfeldChem, Transparent glass-ceramics doped with Cr (III): low-temperature time-resolved spectra and characterization of gahnite and virgilite crystalline phases, Phys. Lett. 133 (4) (1987) 363–367.